

Beam-laser measurements of lifetimes in SiO^+ and N_2^+

T. J. Scholl, R. Cameron, S. D. Rosner, and R. A. Holt

Physics Department, University of Western Ontario, London, Ontario, Canada N6A 3K7

(Received 20 June 1994)

We have constructed a beam-laser lifetime-measuring apparatus and tested it by measuring the well known lifetime of the $v = 0$ level of the $B^2\Sigma_u^+$ state of $^{14}\text{N}_2^+$. Our result of 61.8(5) ns is in excellent agreement with previous high-precision measurements. Employing this technique we performed measurements of the lifetimes of the four lowest vibrational levels of the $B^2\Sigma^+$ state of $^{28}\text{Si}^{16}\text{O}^+$. The results are (in ns) 69.5(6), 72.4(5), 75.2(5), and 78.0(8) for $v = 0, 1, 2,$ and $3,$ respectively.

PACS number(s): 33.70.Fd

I. INTRODUCTION

SiO^+ plays a significant role in the chemistry of diffuse interstellar clouds [1–6], shock-heated dense molecular clouds [7,8], and hot circumstellar regions [9,10]. Although the neutral SiO molecule has been identified in maser or thermal emission from nearly 200 circumstellar sources [11], no direct detection of SiO^+ has been reported. Lovas [12] did consider it as a possible source of the unidentified U86.2 radio line; however, in a recent fast-ion-beam laser spectroscopy study [13] we showed definitively that it could not be the source and we provided a set of precise molecular constants to facilitate optical and radio-frequency searches.

Equally vital to the study of interstellar molecules and in particular to the determination of their abundances is a knowledge of transition probabilities and spontaneous-emission lifetimes. There do not appear to be any experimental or theoretical data in this regard for SiO^+ , apart from the *ab initio* calculation of transition probabilities within and between the $X^2\Sigma^+$ and $A^2\Pi$ states by Werner, Rosmus, and Grimm [14]. We have therefore undertaken a beam-laser lifetime measurement, using a newly constructed apparatus which incorporates all the advantages inherent to the collinear beam-laser technique of Ceyzeriat *et al.* [15]. As a preliminary step to test the reliability of our apparatus, we have made an 0.8%-accuracy measurement of the lifetime of the much-studied $B^2\Sigma_u^+$ state of $^{14}\text{N}_2^+$, obtaining excellent agreement with previous high-precision results. We then measured the lifetimes of four vibrational levels of the $B^2\Sigma^+$ state of $^{28}\text{Si}^{16}\text{O}^+$.

II. EXPERIMENT

The beam-laser method of measuring spontaneous-emission lifetimes, pioneered by Andr a and co-workers [16,17], is a highly reliable and selective technique which produces cascade-free decay curves. Most of the earliest work was undertaken with crossed-beam geometry, where the ions were excited by the pulse of resonant light produced by their motion through the intersection

of the cw laser beam and the ion beam. Later work by Winter and Gaillard [18] employed collinear geometry and the *Doppler switching technique*, which brought the ions into and out of resonance in a Doppler tuning region which was translated along the beam axis. This post-acceleration region was biased with a dc potential so that the fast-moving ions were resonant with the laser frequency only during their transit through this region. Downstream, the spontaneous fluorescence was viewed at right angles by a fixed light collection system. This technique was refined by Ceyzeriat *et al.* [15] to include a modulation of the post-acceleration potential to subtract the background signal. Also, a second resonant Doppler tuning region was added farther downstream and the fluorescence from it was used for normalization to account for fluctuations in laser intensity and ion beam current. In the present work we have further refined the technique of Ceyzeriat *et al.* to provide an improved normalization signal.

The ion accelerator and laser beam source for this experiment were similar to those used in previous spectroscopic measurements and have been described in more detail before [13,19]. The ions were produced in a high-temperature hollow cathode ion source using SiO powder as the source feed for beams of SiO^+ and nitrogen gas for N_2^+ beams. The ions were extracted at an energy of 8 keV, electrostatically focused and mass selected by a Wien filter. After being focused a second time, the ion beam was deflected through a 5° angle by an electric field to overlap the laser beam collinearly and pass through two 6-mm-diam aperture plates separated by 0.85 m. This made it possible to align the axes of the laser beam and ion beam routinely to ± 7 mrad. Finally, the ions were deflected by another electric field into a current monitor. Typical ion currents through the apparatus were 5–6 μA .

Located between the aperture plates was a Doppler tuning region mounted on a translation stage driven by a stepper motor located outside the vacuum. The Doppler tuning region was comprised of an excitation region surrounded on either side by grounded cylinders (see Fig. 1). The excitation region consisted of three post-acceleration electrodes biased to Doppler tune the ions into resonance

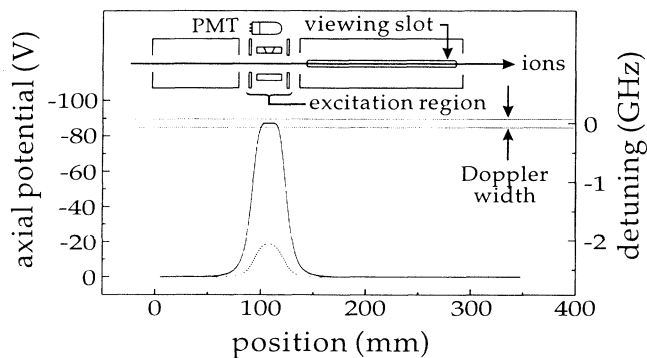


FIG. 1. Schematic drawing of the Doppler tuning region showing the axial potentials. The cylindrically symmetric Doppler tuning region is comprised of three post-acceleration electrodes with grounded cylinders at either side. The potentials on the electrodes were modulated at 1 kHz; the solid and dashed lines represent the axial potential encountered by the ions for either phase of the modulation. The laser frequency was chosen so that the ions were in resonance only for the peak of the solid curve. The Doppler detuning from resonance is shown on the right-hand ordinate. Fluorescence from the Doppler tuning region is viewed by an internal photomultiplier (PMT).

with the laser. The geometry and potential distribution of the excitation region were designed (using the SIMION program [20]) to provide efficient excitation of the ions by maintaining resonance with the laser beam over nearly a 10-mm distance, which corresponds to roughly one lifetime. It is important to realize that the functional form of the exponential decay curve is independent of the temporal resolution of the excitation process, provided one takes care to observe the decay only after all excitation has ceased. This arises from the fundamental property of spontaneous emission that the probability of decay per unit time is independent of the length of time elapsed since excitation. For the same reason, no errors can arise from backlash in the translation stage; this allows us to add together data taken while scanning the Doppler tuning region upstream and downstream.

The grounded cylinder downstream from the excitation region was slotted to permit viewing of the fluorescence by a fixed monochromator as the ions decayed in flight. A spherical mirror was used to double the light-collection efficiency of the monochromator. Decay curves were acquired by translating the Doppler tuning region. The ambient dc magnetic field was canceled by three orthogonal pairs of Helmholtz coils external to the vacuum chamber.

The potentials on the post-acceleration electrodes were modulated at a frequency of 1 kHz using a square wave to bring the ions into and completely out of resonance with the laser light (see Fig. 1). This served two purposes. First, it modulated the intensity of the laser-induced fluorescence in the post-acceleration region; this was viewed by a small photomultiplier internal to the vacuum chamber, which was attached to the post-acceleration region

and translated with it. The photocurrent was monitored by a lock-in amplifier, providing a signal used to normalize the fluorescence decay curve for variations in excitation. Second, this made possible the acquisition of decay curves free of background counts due to ion-neutral species collisions, scattered laser light, and photomultiplier dark noise. Two input channels of a personal computer data acquisition board were used to record the pulses from the monochromator photomultiplier, with each channel gated to one phase of the voltage modulation on the excitation region. A decay curve was acquired as the difference of the two count rates when the ions were in and out of resonance with the laser frequency.

The derivation of the normalization signal is the only major difference between this experimental technique and that of Ceyzeriat *et al.* [15]. That method used the fluorescence from a second unmodulated Doppler tuning region for normalization. In our apparatus, the normalization signal is directly proportional to the fluorescence from the excitation region itself. It thus takes into account not only variations in ion beam current and laser power, but also more subtle effects such as variation in the spatial overlap of the laser beam and the ion beam in the excitation region. Furthermore, the lock-in technique removes the background signal arising from scattered laser light and collisions with residual gas.

For the SiO^+ lifetime measurements, typical ion beam currents of $5 \mu\text{A}$ produced signal count rates of ~ 4000 counts/s for an $F/3.8$ monochromator with 2-mm slits. This slit width corresponded to a resolution of 20 \AA . The background count rate was ~ 250 counts/s, of which ~ 70 counts/s was due to dark noise from the photomultiplier and the majority of the remainder from ion collisions with background gas. The background pressure in the interaction region of the system was 4×10^{-7} Torr. For the N_2^+ measurements, the signal and background count rates were ~ 4500 and ~ 750 counts/s, respectively, with an ion current of $6.5 \mu\text{A}$.

For the $\Delta v = 0$, $B^2\Sigma^+ - X^2\Sigma^+$ bands of $^{28}\text{Si}^{16}\text{O}^+$ the excitation light at $\sim 385 \text{ nm}$ was produced by intracavity frequency doubling of a single frequency cw Ti-sapphire ring laser. The typical output power was 60 mW. The (0,1) band of the $B^2\Sigma_u^+ - X^2\Sigma_g^+$ of $^{14}\text{N}_2^+$ was excited with light from a uv-pumped cw ring dye laser with Stilbene 420 dye. The single frequency output power was $\sim 200 \text{ mW}$ at 428 nm. For all measurements, the laser beams were loosely collimated by a 1.5-m focal length lens before entering the vacuum. The entrance and exit windows were at Brewster's angle and two internal baffles were located after the entrance window to reduce scattered laser light. The laser beam direction was defined by two fixed apertures separated by $\sim 3.8 \text{ m}$, located on either side of the vacuum system to position the laser beam accurately relative to the apparatus.

The single frequency ring lasers had $\sim 1\text{-MHz}$ linewidths and were frequency stabilized to better than 20 MHz/h. The 60-V anode-cathode potential of the ion source was fixed by a voltage-stabilized power supply and the discharge current (60 mA) was kept constant within 10% by manual adjustment of the filament heating. Slow drifts away from exact resonance with the peak

of the Doppler distribution, caused either by laser frequency drift or ion beam velocity drift, could be monitored and corrected by the recorded normalization signal. The Doppler widths for N_2^+ and SiO^+ were 170 MHz and 150 MHz, respectively; for collinear geometry this corresponds to a 5-eV energy spread of the ion beam. Thus, with this selective excitation, even the hyperfine structure of N_2^+ was well resolved and, in principle, the lifetime measurements could be easily made as a function of rotational quantum number or for different hyperfine components. This is of value in cases where the lifetime is affected by predissociation mediated by hyperfine interactions [21].

A decay curve was acquired by stepping the position of the Doppler tuning region while recording the two gated fluorescence signals from the monochromator, the normalization signal from the internal photomultiplier, the laser power, and the ion beam current. For a typical decay curve, the Doppler tuning region was translated in steps of 1.27 mm, dwelling for 3 s at each position. Scans began from a position ~ 38 mm from the center of the post-acceleration region (equivalent to 2.9 lifetimes for SiO^+ and 2.6 for N_2^+) and were made back and forth over a distance of 86 mm (6.5 lifetimes for SiO^+ and 5.9 for N_2^+). Twelve separate decay curves were accumulated for each vibrational band. In addition to the decay curves, a spectrum measuring the laboratory frequency of the optical transition was acquired before and after each series of lifetime measurements to calibrate the ion velocity using the relativistic Doppler formula. The ability to determine the ion velocity with negligible uncertainty is a major advantage of all collinear beam-laser techniques.

III. RESULTS

A. N_2^+ lifetime analysis

The fitting procedure first normalized the individual fluorescence decay curves using the lock-in signal from the internal photomultiplier. The statistical weight of a data point was determined as follows. Before normalization, the net signal is the difference of two gated signals obeying Poisson statistics; thus the uncertainty was estimated as the square root of the sum of the gated signals. An estimate of the uncertainty due to noise in the normalization signal was added in quadrature (see below). Nonlinear least-squares curve fitting was used to determine the amplitude, exponential decay constant, and any residual background not eliminated by the gating technique. The background was determined to be 51 ± 71 counts, which is consistent with zero. The 12 data sets for N_2^+ were analyzed individually as an internal check on the consistency of the data and also analyzed summed together. The results of these individual fits are shown in Table I. The standard deviation of the mean of the 12 measurements was 0.42 ns and the weighted average of the lifetime was 61.7(3) ns. The fit to the summed decay curves produced a lifetime of 61.8(3) ns and a χ^2 per degree of freedom χ_{reduced}^2 of 1.03 (see Fig. 2). The excellent agreement between the internal and external values

TABLE I. Determination of the lifetime of the $v = 0$ level of the $B^2\Sigma_u^+$ state of $^{14}\text{N}_2^+$ from individual normalized fluorescence decay curves.

Lifetime (ns)	χ_{reduced}^2
61.8 ± 0.7	1.1
61.8 ± 1.0	1.0
61.7 ± 0.9	0.8
62.1 ± 0.9	1.0
61.8 ± 0.8	1.2
60.2 ± 0.8	1.2
58.9 ± 1.2	1.2
63.4 ± 1.3	1.2
62.0 ± 1.4	0.8
64.4 ± 1.5	1.0
62.1 ± 1.2	1.3
63.4 ± 1.3	1.0

gives us confidence in our estimates of the statistical uncertainty.

In addition to the statistical uncertainty, several other random and systematic errors must be considered. The conversion from distance to time was made by calculating β (speed of ions relative to that of light) using the optical spectra taken before and after the lifetime measurement. The absolute wave number of the $P_2(15)$, $J'' = 14\frac{1}{2}$, $F'' = 13\frac{1}{2}$ transition of the $B^2\Sigma_u^+ - X^2\Sigma_g^+(0,1)$ band was measured in the laboratory frame to better than a part in 10^7 using the Aimé-Cotton Te_2 atlas as the reference [22]. The wave number of this transition is known to about the same precision from previous studies [19]. These two wave numbers yield an 8 parts in 10^5 measurement of β , which leads to a completely

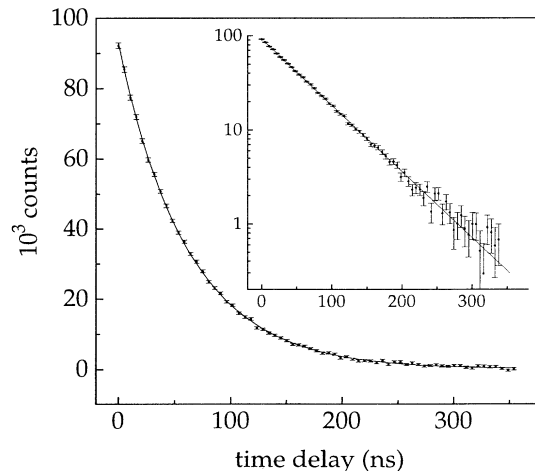


FIG. 2. Least-squares fit to summed and normalized fluorescence decay curves for the $v = 0$ level of the $B^2\Sigma_u^+$ state of $^{14}\text{N}_2^+$. The abscissa is measured relative to the first channel and a constant background of 51 counts, determined from the fit, has been subtracted from the signal. The χ^2 per degree of freedom was 1.03. The inset is a semilogarithmic plot of the same data and fit.

negligible contribution to the uncertainty of the lifetime measurement.

Using $5 \times 10^{-15} \text{ cm}^2$ as an upper limit on the quenching cross section for N_2^+ [23,24], the mean free path at our background pressure of 4×10^{-7} Torr would be ~ 154 m. For $\beta = 7.89 \times 10^{-4}$ the collisional quenching rate is $1.53 \times 10^3 \text{ s}^{-1}$, representing a negligible correction of 0.006 ns to the lifetime. Furthermore, lifetime measurements made with changes in background pressures ranging over more than an order of magnitude showed no effects of collisional quenching within experimental error. Since the spontaneous decay of the ions was viewed in a field-free region maintained by the grounded cylinder and the Helmholtz coils, corrections for the Stark effect or quantum beats were also negligible.

The largest systematic error in beam-laser measurements of lifetimes often arises from spatial and temporal variation of the excitation of the transition as the decay curve is acquired. It is necessary to maintain constant laser power, frequency, and transverse mode distribution, ion current, velocity, and cross sectional distribution, as well as unvarying overlap of the two beams during the entire acquisition period. In practice, we found that about half of the variation of the normalization signal could be explained by the recorded variations of the ion beam current and laser power, mostly due to the former. It was thus essential to have the normalization signal to correct the decay curve. The normalization signal on average varied about 5% over a scan. Analyzing the data with no normalization shifted the lifetime by 5% and yielded a χ^2 probability of 11%. With correction by the normalization signal, the χ^2 probability increased to 40%.

Small systematic errors in lifetime measurements can sometimes be revealed by analyzing a subset of the data that includes only data above a given channel, a procedure known as tail fitting. Figure 3 shows the variation in the lifetime as the starting channel for the tail fit is systematically increased; the background and amplitude were fixed at the values obtained for the entire data set. The lifetime remained essentially constant and within the

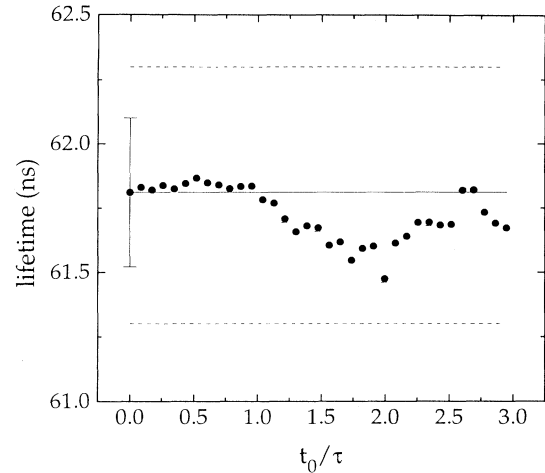


FIG. 3. Tail fitting analysis of the lifetime τ of the $v = 0$ level of the $B^2\Sigma_u^+$ state of $^{14}\text{N}_2^+$. The quantity t_0 is the time corresponding to the initial channel included in the least-squares fit for the lifetime (measured from the first channel of data). The error bar represents one standard deviation of the statistical uncertainty in the lifetime from fitting all the data. The background and amplitude for the fit to the decay curve were held fixed as t_0 was varied out to three lifetimes. The dashed lines represent the total estimated uncertainty of the lifetime including three times the uncertainty introduced during normalization added in quadrature to the statistical uncertainty in the least-squares fit.

uncertainty bounds as the first three lifetimes of data were ignored.

The statistical uncertainty in the normalization signal was determined from the observed scatter about linear regression fits to small portions of this signal. This was then numerically propagated into the lifetime by changing in turn the data in each channel of the normaliza-

TABLE II. Summary of high-precision measurements of the lifetime of the $v = 0$ level of the $B^2\Sigma_u^+$ state of $^{14}\text{N}_2^+$. Methods used are PE, pulsed electrons; PP, pulsed protons; BG, beam gas; IEPDC, inelastic electron-photon delayed coincidence; HFD, high-frequency deflection; and BL, beam laser. N is the rotational quantum number.

Author(s)	Reference	Method	N	Pressure (mbar)	Lifetime (ns)
Sebacher	[25]	PE		1.5×10^{-1}	65.0 ± 2.0
Nichols and Wilson	[26]	PP		65-550	65.9 ± 1.0
Desesquelles <i>et al.</i>	[27]	BG		1×10^{-5}	66.0 ± 1.4
Gray <i>et al.</i>	[28]	PE		1.5×10^{-4}	61.3 ± 0.8
Dotchin <i>et al.</i>	[29]	PP		$(1 \times 10^{-3}) - (2.5 \times 10^{-1})$	60.4 ± 0.4
Bingham	[30]	PP		$1 \times 10^{-2} - 1$	60.7 ± 1.3
Smith <i>et al.</i>	[31]	IEPDC		2.5×10^{-4}	60.6 ± 0.6
Erman	[24]	HFD	9-15	$< 1 \times 10^{-3}$	62.4 ± 0.3
Remy and Dumont	[32]	PE	6-18	$(7 \times 10^{-5}) - (1 \times 10^{-3})$	61.5 ± 0.4
Schmoranzner <i>et al.</i>	[33]	BL	8-13	1×10^{-6}	61.35 ± 0.29
This work		BL	14	4×10^{-7}	61.8 ± 0.5

tion by one standard deviation and repeating the least-squares lifetime analysis with the altered normalization. This procedure produced an average estimate of the contribution to the uncertainty in the lifetime of 0.13 ns. As a cautious overestimate of any systematic errors in the experiment due to variations in ion excitation which were not removed by normalization with the internal photomultiplier signal we have tripled this statistical uncertainty. Adding this error in quadrature with the statistical uncertainty, the final result for the lifetime is 61.8(5) ns. This estimate of the total uncertainty is indicated by dashed lines in Fig. 3.

The lifetime of the $v = 0$ level of the $B^2\Sigma_u^+$ state of $^{14}\text{N}_2^+$ has been carefully measured by a variety of techniques [24–33], making it an excellent calibration test of this apparatus. Table II summarizes the most precise of the previous results. Our measurement on a single rotational level has the highest resolution and complete selectivity. It is meaningful to compare it with lower-resolution results that sum over a range of rotational levels because they are all in a region far from localized perturbations due to the $A^2\Pi_u$ level [19]. It is evident that there is close agreement among the most recent high-precision results, which gives us confidence that our technique is capable of lifetime measurements with better than 1% accuracy.

B. SiO⁺ lifetime analysis

The data analysis for the $v = 0, 1, 2, 3$ levels of the $B^2\Sigma^+$ state of SiO⁺ was undertaken in the manner previously described for N₂⁺. The collisional background was smaller by a factor of more than 3, resulting in lower statistical uncertainty. The summed normalized decay curve for $v = 0$ is shown in Fig. 4. The fitted back-

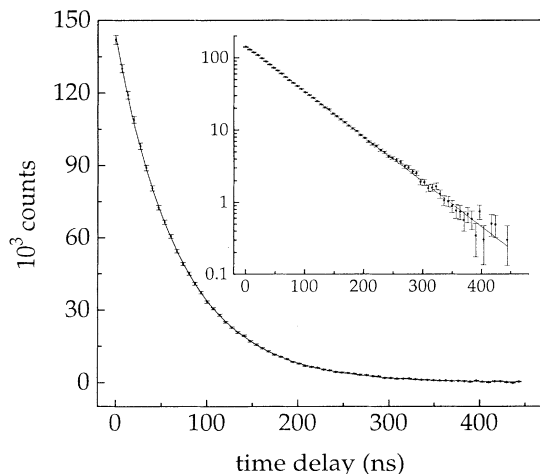


FIG. 4. Least-squares fit to summed and normalized fluorescence decay curves for the $v = 0$ level of the $B^2\Sigma^+$ state of $^{28}\text{Si}^{16}\text{O}^+$. The lifetime was determined to be 69.5(6) ns. The abscissa is measured relative to the first channel and a constant background of -3 counts, determined from the fit, has been subtracted from the signal. The χ^2 per degree of freedom was 0.90. The inset is a semilogarithmic plot of the same data and fit.

TABLE III. Lifetime measurements of the $B^2\Sigma^+$ state of $^{28}\text{Si}^{16}\text{O}^+$ as a function of vibrational level. All uncertainties represent one standard deviation. N is the rotational quantum number.

v	N	τ (ns)	$\Delta\tau_{\text{statistical}}$ (ns)	$\Delta\tau_{\text{normalization}}$ (ns)	$\Delta\tau_{\text{total}}$ (ns)	χ_{reduced}^2
0	41	69.5	0.2	0.6	0.6	0.9
1	40	72.4	0.3	0.5	0.5	1.1
2	39	75.2	0.4	0.3	0.5	1.3
3	29	78.0	0.6	0.5	0.8	0.9

ground was -3 ± 39 counts. The lifetime measurements for these levels are shown in Table III. There is a clear trend of significant increase in lifetime with increasing vibrational level.

No previous measurements or theoretical predictions exist for comparison, but other results in related molecules are available. In particular, the CO⁺ molecular ion, which has a similar valence structure outside the closed-shell core, has been the subject of a theoretical and experimental study by Marian *et al.* [34]. Figure 5 plots our SiO⁺ data together with the measured and calculated CO⁺ results of Marian *et al.* It is evident that both molecules exhibit similar behavior and furthermore that the theory accounts for it in the case of CO⁺ (apart from an overall 10% discrepancy in the absolute values). The “state-averaged complete active space self-consistent-field-multireference configuration interaction” calculations of Marian *et al.* provide an insight into the origin of the strong vibrational de-

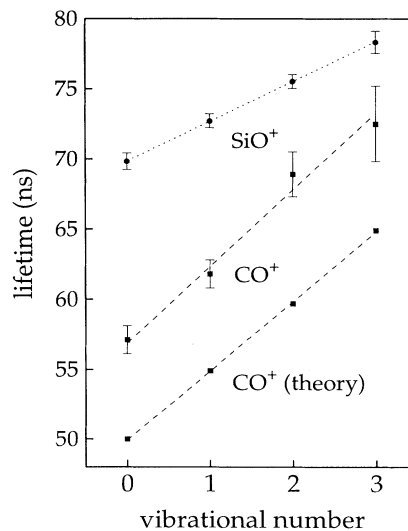


FIG. 5. Vibrational dependence of B -state lifetimes in SiO⁺ and CO⁺. Measurements of the lifetimes of the first four vibrational levels of the $B^2\Sigma^+$ state of $^{28}\text{Si}^{16}\text{O}^+$ are compared with the measurements and theoretical predictions of Marian *et al.* for the $B^2\Sigma^+$ state of CO⁺. The dashed lines are linear regression fits.

pendence of the B -state lifetime. In contrast to the $X^2\Sigma^+$ ground state, which is well described by the single $1\sigma^2 2\sigma^2 3\sigma^2 4\sigma^2 1\pi^4 5\sigma^1$ configuration at all relevant internuclear distances, the $B^2\Sigma^+$ configuration changes significantly as the internuclear separation is increased. Near the equilibrium distance, it is predominantly $1\sigma^2 2\sigma^2 3\sigma^2 4\sigma^1 1\pi^4 5\sigma^2$, but as the distance increases, there is a greater admixture of another low-lying configuration $1\sigma^2 2\sigma^2 3\sigma^2 4\sigma^2 1\pi^3 5\sigma^1 2\pi^1$, which is also singly excited with respect to the ground-state configuration. This configuration enters the B -state wave function with a sign opposite to that of the $\dots 4\sigma^1 1\pi^4 5\sigma^2$ configuration. The resulting cancellation of contributions to the electric dipole transition moment leads to a rapid decrease with increasing internuclear distance, and hence with increasing vibrational number, as a result of anharmonicity in the potential [34]. In the SiO^+ case, similar calculations should be possible and it is reasonable to suppose that a similar mechanism is the cause of the behavior we have observed. Indeed, measurements such as these can serve as a valuable test of *ab initio* calculations, which can then be trusted to provide absolute transition probabilities and lifetimes for molecules which may be difficult to study experimentally.

IV. CONCLUSIONS

We have tested our modified beam-laser lifetime measuring technique with a measurement of the lifetime of the $v = 0$ level of the $B^2\Sigma_u^+$ state of N_2^+ which agrees with previous precision beam-laser measurements. The use of collinear geometry in this beam-laser technique provides precise knowledge of the ion velocity and excellent spectroscopic selectivity. Our experimental design provides a true normalization signal, background elimination, and efficient excitation. This apparatus has then been used to measure the lifetime of the first four vibrational levels of the $B^2\Sigma^+$ state of SiO^+ , which were previously unknown, to better than 1%.

ACKNOWLEDGMENTS

We are pleased to thank the Natural Sciences and Engineering Research Council of Canada, the Centre of Excellence for Molecular and Interfacial Dynamics, and the Academic Development Fund of the University of Western Ontario for financial support. We would also like to thank Mr. H. Chen for valuable assistance with the electronics.

-
- [1] J. L. Turner and A. Dalgarno, *Astrophys. J.* **213**, 386 (1977).
 - [2] T. J. Millar, *Astrophys. Space Sci.* **72**, 509 (1980).
 - [3] S. S. Prasad and W. T. Huntress, *Astrophys. J. Suppl.* **43**, 1 (1980).
 - [4] E. Herbst, T. J. Millar, S. Wlodek, and D. K. Bohme, *Astron. Astrophys.* **222**, 205 (1989).
 - [5] S. P. Tarafdar and A. Dalgarno, *Astron. Astrophys.* **232**, 239 (1990).
 - [6] W. D. Langer and A. E. Glassgold, *Astrophys. J.* **352**, 123 (1990).
 - [7] T. W. Hartquist, M. Oppenheimer, and A. Dalgarno, *Astrophys. J.* **236**, 182 (1980).
 - [8] D. A. Neufeld and A. Dalgarno, *Astrophys. J.* **340**, 869 (1989); **344**, 251 (1989).
 - [9] J. M. Scalo and D. B. Slavsky, *Astrophys. J. Lett.* **239**, L73 (1980).
 - [10] P. E. S. Clegg, L. J. van Ijzendoorn, and L. J. Allamandola, *Mon. Not. R. Astron. Soc.* **203**, 125 (1983).
 - [11] D. Engels and A. Heske, *Astron. Astrophys. Suppl.* **81**, 323 (1989).
 - [12] F. J. Lovas, *Astrophys. J.* **193**, 265 (1974).
 - [13] L. Zhang, R. Cameron, R. A. Holt, T. J. Scholl, and S. D. Rosner, *Astrophys. J.* **418**, 307 (1993).
 - [14] H.-J. Werner, P. Rosmus, and M. Grimm, *Chem. Phys.* **73**, 169 (1982).
 - [15] P. Ceyzeriat, D. J. Pegg, M. Carré, M. Druetta, and M. L. Gaillard, *J. Opt. Soc. Am.* **70**, 901 (1980).
 - [16] H. J. Andrä, A. Gaupp, K. Tillmann, and W. Wittmann, *Nucl. Instrum. Methods* **110**, 453 (1973).
 - [17] H. J. Andrä, in *Beam-Foil Spectroscopy*, edited by I. A. Sellin and D. J. Pegg (Plenum, New York, 1976), Vol. 2, p. 835.
 - [18] H. Winter and M. Gaillard, *Z. Phys. A* **281**, 311 (1977).
 - [19] T. J. Scholl, A. W. Taylor, R. A. Holt, and S. D. Rosner, *J. Mol. Spectrosc.* **152**, 398 (1992).
 - [20] Available from David A. Dahl, MS 2208, Idaho National Engineering Laboratory, EG&G Idaho, Inc., P.O. Box 1625, Idaho Falls, ID 83415.
 - [21] J. L. Booth, I. Ozier, and F. W. Dalby, *Phys. Rev. Lett.* **72**, 2371 (1994).
 - [22] J. Cariou and P. Luc, *Atlas du Spectre d'Absorption de la Molécule de Tellure* (Laboratoire Aimé-Cotton, CNRS II, Orsay, 1980).
 - [23] A. W. Johnson and R. G. Fowler, *J. Chem. Phys.* **53**, 65 (1970).
 - [24] P. Erman, *Phys. Scr.* **11**, 65 (1975).
 - [25] D. D. Sebach, *J. Chem. Phys.* **42**, 1368 (1965).
 - [26] L. L. Nichols and W. E. Wilson, *Astrophys. Opt.* **7**, 167 (1968).
 - [27] J. Desesquelles, M. Dufay, and M. C. Poulizac, *Phys. Lett.* **27A**, 96 (1968).
 - [28] D. Gray, J. L. Morack, and T. D. Roberts, *Phys. Lett.* **37A**, 25 (1971).
 - [29] L. W. Dotchin, E. L. Chupp, and D. J. Pegg, *J. Chem. Phys.* **59**, 3960 (1973).
 - [30] F. W. Bingham, *Bull. Am. Phys. Soc.* **18**, 609 (1973).
 - [31] A. A. J. Smith, F. H. Read, and R. E. Imhof, *J. Phys. B* **8**, 2869 (1975).
 - [32] F. Remy and M. N. Dumont, *J. Quant. Spectrosc. Radiat. Transfer* **20**, 217 (1978).
 - [33] H. Schmoranz, P. Hartmetz, D. Marger, and J. Dudda, *J. Phys. B* **22**, 1761 (1989).
 - [34] C. M. Marian, M. Larsson, B. J. Olsson, and P. Sigray, *Chem. Phys.* **130**, 361 (1989).